



Ultracool dwarfs in deep extragalactic surveys using the virtual observatory: ALHAMBRA and COSMOS

E. Solano, M. C. Gálvez-Ortiz, E. L. Martín, I. M. Gómez Muñoz, C. Rodrigo, A. J. Burgasser, N. Lodieu, V. J. S. Béjar, N. Huélamo, M. Morales-Calderón, et al.

► To cite this version:

E. Solano, M. C. Gálvez-Ortiz, E. L. Martín, I. M. Gómez Muñoz, C. Rodrigo, et al.. Ultracool dwarfs in deep extragalactic surveys using the virtual observatory: ALHAMBRA and COSMOS. Monthly Notices of the Royal Astronomical Society, 2021, 501, pp.281-290. 10.1093/mnras/staa3423 . insu-03678891

HAL Id: insu-03678891

<https://insu.hal.science/insu-03678891>

Submitted on 2 May 2023

HAL is a multi-disciplinary open access archive for the deposit and dissemination of scientific research documents, whether they are published or not. The documents may come from teaching and research institutions in France or abroad, or from public or private research centers.

L'archive ouverte pluridisciplinaire **HAL**, est destinée au dépôt et à la diffusion de documents scientifiques de niveau recherche, publiés ou non, émanant des établissements d'enseignement et de recherche français ou étrangers, des laboratoires publics ou privés.

Ultracool dwarfs in deep extragalactic surveys using the virtual observatory: ALHAMBRA and COSMOS

E. Solano,¹★ M. C. Gálvez-Ortiz,² E. L. Martín,^{3,4,5} I. M. Gómez Muñoz,⁶ C. Rodrigo,¹
A. J. Burgasser,⁷ N. Lodieu,^{3,4} V. J. S. Béjar,^{3,4} N. Huélamo,¹ M. Morales-Calderón¹ and H. Bouy⁸

¹Centro de Astrobiología (CSIC-INTA), ESAC Campus, Camino Bajo del Castillo s/n, E-28692 Madrid, Spain

²Suffolk University, Madrid Campus, C/ Valle de la Viña 3, E-28003 Madrid, Spain

³Instituto de Astrofísica de Canarias (IAC), Calle Vía Láctea s/n, E-38200 La Laguna, Tenerife, Spain

⁴Departamento de Astrofísica, Universidad de La Laguna (ULL), E-38206 La Laguna, Tenerife, Spain

⁵Consejo Superior de Investigaciones Científicas, E-28006 Madrid, Spain

⁶Universidad Internacional de Valencia. Carrer del Pintor Sorolla 21, E-46002 Valencia, Spain

⁷Center for Astrophysics and Space Science, University of California San Diego, 9500 Gilman Drive, La Jolla, CA 92092, USA

⁸Laboratoire d'astrophysique de Bordeaux, University of Bordeaux, CNRS, B18N, Allée Geoffroy Saint-Hilaire, F-33615 Pessac, France

Accepted 2020 October 26. Received 2020 October 23; in original form 2020 March 23

ABSTRACT

Ultracool dwarfs (UCDs) encompass a wide variety of compact stellar-like objects with spectra classified as late-M, L, T, and Y. Most of them have been discovered using wide-field imaging surveys. The Virtual Observatory (VO) has proven to be of great utility to efficiently exploit these astronomical resources. We aim to validate a VO methodology designed to discover and characterize UCDs in deep extragalactic surveys like Advance Large Homogeneous Area Medium-Band Redshift Astronomical (ALHAMBRA) and Cosmological Evolution Survey (COSMOS). Three complimentary searches based on parallaxes, proper motions and colours, respectively, were carried out. A total of 897 candidate UCDs were found, with only 16 previously reported in SIMBAD. Most of the new UCDs reported here are likely late-M and L dwarfs because of the limitations imposed by the utilization of optical (*Gaia* DR2 and *r*-band) data. We complement ALHAMBRA and COSMOS photometry with other catalogues in the optical and infrared using VOSA, a VO tool that estimates effective temperatures from the spectral energy distribution fitting to collections of theoretical models. The agreement between the number of UCDs found in the COSMOS field and theoretical estimations together with the low false-negative rate (known UCDs not discovered in our search) validates the methodology proposed in this work, which will be used in the forthcoming wide and deep surveys provided by the Euclid space mission. Simulations of Euclid number counts for UCDs detectable in different photometric passbands are presented for a wide survey area of 15 000 deg², and the limitations of applicability of Euclid data to detect UCDs using the methods employed in this paper are discussed.

Key words: surveys – virtual observatory tools – brown dwarfs – stars: low-mass.

1 INTRODUCTION

Ultracool dwarfs (UCDs) are defined as objects with spectral types M7 V or later and comprise very low-mass stars, brown dwarfs (BDs), and planetary-mass objects. They represent about 15 per cent of the stellar population in the solar neighbourhood (Henry et al. 2006) and their lifetimes make them the longest-lived not evolved objects of the universe. The M7 V spectral type is just below the substellar boundary in the benchmark Pleiades cluster (e.g. Martín, Rebolo & Zapatero-Osorio 1996; Rebolo et al. 1996), and it marks the beginning of a variety of changes that are seen to happen with decreasing effective temperature, in particular, the appearance of dust clouds and the marked increase of pressure-broadened neutral atomic lines of alkali elements (e.g. Jones & Tsuji 1997; Martín et al. 1997; Kirkpatrick et al. 1999; Helling et al. 2008).

In addition to be key elements to properly understand the physical processes at the stellar/substellar boundary, UCDs are excellent candidates for exoplanet searches. As they are much fainter and smaller than solar-like stars, it is much easier to detect low-mass rocky planets orbiting around them (Martín et al. 2013). TRAPPIST-1 (Gillon et al. 2017) has been the first successful example of this type of planetary system.

Not many studies of stellar and substellar objects in extragalactic surveys can be found in the literature. The search of BDs in the UKIDSS DXS and UDS surveys by Lodieu et al. (2009) and the pioneering work by Cuby et al. (1999) using the NTT Deep Field and Liu et al. (2002) using the IfA Deep Survey are some of the few exceptions to this. In fact, UCDs are normally treated as contaminants since, at high-redshift, galaxies and UCDs show similar colours in the near-IR (Wilkins, Stanway & Bremer 2014; Ryan & Reid 2016). This, together with the photometric depth of the extragalactic surveys, makes them very interesting niches for the

★ E-mail: esm@cab.inta-csic.es

discovery of UCDs. In this paper, we use the ALHAMBRA (Advance Large Homogeneous Area Medium-Band Redshift Astronomical) and COSMOS surveys to discover and characterize new UCDs. These two extragalactic surveys have a relatively large field of view and low extinction, which facilitates the discovery a significant number of UCDs and the determination of their physical parameters. Our main goal is to assess the effectiveness of a Virtual Observatory (VO)-based methodology that could be used in future, deeper and larger surveys like those planned with the Euclid¹ space mission.

ALHAMBRA (Moles et al. 2008) is a deep photometric survey aimed at providing precise photometric redshifts and information on the spectral energy distributions (SEDs) of thousands of galaxies and active galactic nuclei. ALHAMBRA was conducted in eight different regions of the sky, covering a total area of 4 deg² and including overlapping sections of COSMOS, DEEP2, ELAIS, GOODS-N, SDSS, and Groth survey fields. Observations were made at Calar Alto Observatory with the 3.5-m telescope using LAICA (optical) and Omega-2000 (near-IR) instruments. These observations provided photometric information in 20 contiguous, equal-width, medium-band filters from 3500 to 9700 Å plus the standard *J*, *H*, and *Ks* near-IR bands. The ALHAMBRA filter set and associated limiting magnitudes are given in table 3 of Molino et al. (2014).

The COSMOS project pioneered the study of galactic structures at intermediate to high redshifts as well as the evolution of the galaxy and AGN populations, thanks to the unique combination of a large area and precise photometric redshifts. In this work, we made use of the COSMOS2015² catalogue, which contains photometric information for 1.182.108 sources over the 2 deg² COSMOS field. This version of the COSMOS catalogue was improved from previous versions by the addition of new *YJHKs* images from the UltraVISTA-DR2 survey, *Y*-band images from Subaru/Hyper-Suprime-Cam, and infrared data from the Spitzer Large Area Survey with the Hyper-Suprime-Cam Spitzer legacy program. The COSMOS photometric bands and the averaged limiting magnitudes are given in table 1 of Laigle et al. (2016). All ALHAMBRA and COSMOS magnitudes are given in the AB system.

This paper is organized as follows: In Section 2, we describe the methodology, we have followed to separate stars from galaxies and to identify candidate UCDs among the stellar sources. In Section 3, we assess the robustness of our methodology by studying the fraction of known UCDs that have been recovered. Section 4 presents the spectroscopic analysis made to confirm the UCD nature of some of our candidates. Section 5 deals with simulations of UCD number counts in the Euclid surveys and how the lessons learnt from this work may be used to optimize the identification of UCDs in those fields, and, finally, Section 6 contains the conclusions of this work.

2 METHODOLOGY

2.1 Sample selection

The ALHAMBRA final catalogue³ provides astrometric, morphometric, photometric, redshift, and quality information for 438 661 sources (see the *Documentation* section for a detailed description of the catalogue contents).

We first applied a morphometric filter to keep only stellar objects. For this, we made use of the *stell* and *Stellar_Flag* parameters with

the conditions $stell \geq 0.5$ and $Stellar_Flag \geq 0.5$ (Molino et al. 2014). *stell* is the stellarity parameter implemented in SExtractor with values ranging from 0 (galaxy) to 1 (star). *Stellar_Flag* represents a source-by-source statistical classification among stars and galaxies, as described in Molino et al. (2014). Later, we used a photometric flag to remove saturated objects (*Satur_Flag* = 0), and, finally, we discarded bona fide extragalactic objects by keeping sources with values in the redshift column ($zb - 1$) smaller than 0.5. This parameter can have associated large uncertainties so, in order not to lose any potential candidate UCD, we decided to adopt this very conservative criterion. This gave us a list of 54 611 objects.

In the COSMOS catalogue, we applied a morphometric filter using the keyword *TYPE* set to 1 and *zphot* equal to 0 or -99.9 . This way we ended up with 37 069 objects.

2.2 Hertzsprung–Russell diagram

We cross-matched the 54 611 ALHAMBRA objects with *Gaia* DR2 using a 3 arcsec radius. We kept only counterparts with relative errors of less than 10 per cent in *G* and G_{RP} and less than 20 per cent in parallax. The absolute *Gaia* magnitude in the *G* band for individual stars was estimated using

$$M_G = G + 5 \log \varpi + 5, \quad (1)$$

where ϖ is the parallax in arcseconds. In our case, the inverse of the parallax is a reliable distance estimator because we kept only sources with relative errors in parallax lower than 20 per cent (Luri et al. 2018).

After the cross-match, we ended up with 1 548 stellar sources. A preliminary selection of UCDs was done using the updated version⁴ of table 5 in Pecaut & Mamajek (2013) taking a conservative value of $G - G_{RP} > 1.3$ (corresponding, according to this table, to M5 V). This gave us 119 candidate UCDs. These candidates were plotted on top of a Hertzsprung–Russell diagram (HRD) built with all the *Gaia* DR2 objects at less than 100 pc and good *G*, G_{RP} photometry (Fig. 1). This diagram is similar to that shown in fig. 6 of *Gaia* Collaboration et al. (2018).

We made use of VOSA⁵ (Bayo et al. 2008) to estimate effective temperatures of these 119 objects. VOSA computes physical parameters by fitting the observational SED to different collections of theoretical models. In our analysis, we made use of the BT-Settl collection (Allard, Homeier & Freytag 2012). Gravity and metallicity were restricted to the ranges $\log g$: 4.5–6 and $[M/H]$: -0.5 – $+0.5$, respectively. No extinction correction was used as low extinction was the first and basic criterion to select the ALHAMBRA fields (Moles et al. 2008). An example of a VOSA SED fitting can be found in Fig. 2.

To calibrate the effective temperatures obtained from the comparison with the BT-Settl models using VOSA with spectral types, we use the list of spectroscopically confirmed M dwarfs compiled by West et al. (2011). The mean effective temperature as a function of the spectral type as well as the standard deviations are given in Table 1. According to this table, we adopt for UCDs a conservative value of $T_{\text{eff}} \leq 2900$ K. Only sources with good SED fitting ($vgfb < 15$) were kept. $vgfb$ is a modified χ^2 , calculated by forcing ΔF_{obs} to be larger than $0.1 \times F_{\text{obs}}$, where ΔF_{obs} is the error in the observed flux (F_{obs}). This parameter is particularly useful when the photometric errors of any of the catalogues used to build the SED are underestimated.

¹<http://sci.esa.int/euclid/>

²<http://cdsarc.u-strasbg.fr/viz-bin/cat/J/ApJS/224/24>

³<http://svo2.cab.inta-csic.es/vocats/alhambra/>

⁴<https://www.pas.rochester.edu/~emamajek/>

⁵<http://svo2.cab.inta-csic.es/theory/vosa/>

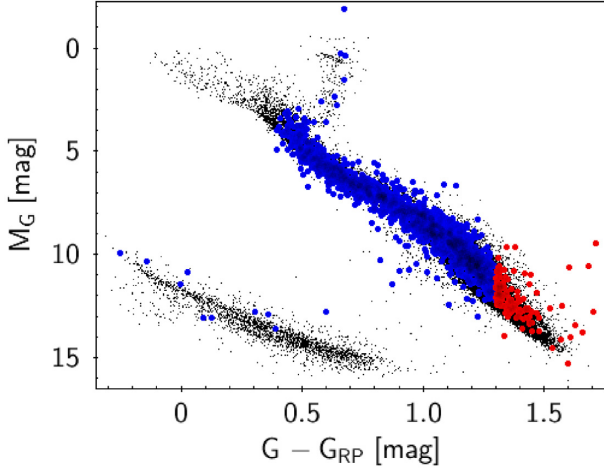


Figure 1. Colour–magnitude diagram built using *Gaia* DR2 sources with parallaxes larger than 10 mas and good photometry (small black dots). Large blue dots indicate the position of the 1 548 ALHAMBRA stellar (dwarfs, giants, and white dwarfs) sources. Candidate UCDs defined as objects with $G - G_{RP} > 1.3$ (119 objects) are overplotted in red. A similar distribution is obtained if COSMOS data are used.

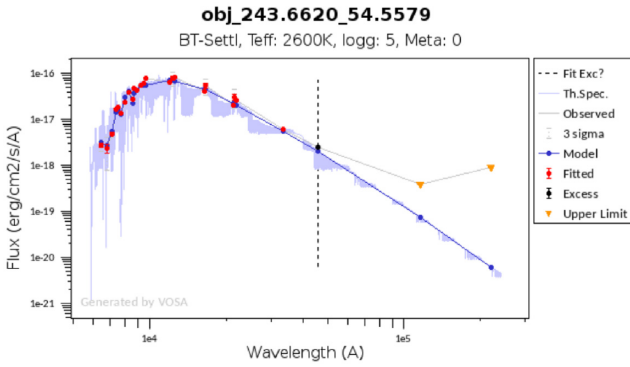


Figure 2. Example of an SED fitting as generated by VOSA. The blue spectrum represents the theoretical model that fits best, while red dots represent the observed photometry. The inverted yellow triangle indicates that the photometric value corresponds to an upper limit.

Table 1. Effective temperatures calculated using BT-Settl models as a function of the spectral type of the objects given in (West et al. 2011).

Spectral Type	Number of objects	Effective temperature (K)	Standard deviation (K)
M5	3901	3213	206
M6	5645	3057	106
M7	5824	2959	152
M8	1682	2715	157
M9	891	2596	162

$v_{\text{gfb}} < 15$ is a reliable indicator of good fit. After applying these conditions we ended up with 30 sources.

Similarly, we cross-matched the 37 069 objects in the COSMOS sample with *Gaia* DR2 using a 3 arcsec radius. We found 207 fulfilling the conditions on parallaxes and photometry, out of which only one (COSMOS 998096) has $T_{\text{eff}} \leq 2900$ K.

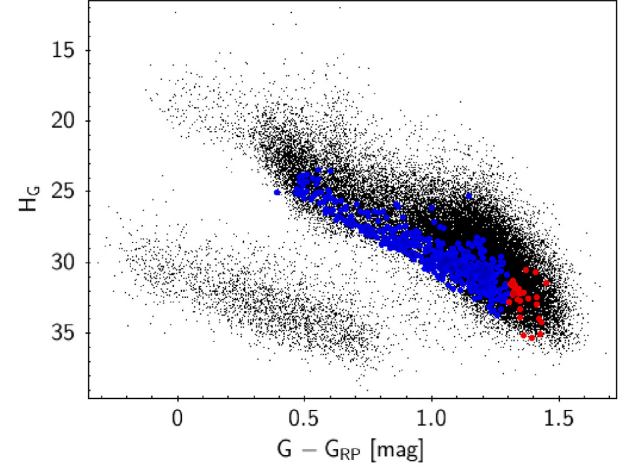


Figure 3. Reduced proper motion–colour diagram. In black, we plot the objects used to build the Hertzsprung–Russell diagram in Fig. 1. Blue circles represent the 462 ALHAMBRA sources that lie in the expected locus for dwarfs. Candidate UCDs defined as objects with $G - G_{RP} > 1.3$ (29 objects) are overplotted in red. A similar distribution is obtained if COSMOS data are used.

A mean value of ~ 170 pc was obtained for the 31 sources (30 ALHAMBRA + 1 COSMOS) with good parallaxes, with the closest and farthest objects at 70 and 350 pc, respectively.

2.3 Proper motions

Proper motions can be used to discriminate between galaxies and stars because extragalactic objects must have negligible values. For instance, M31, the nearest galaxy to the Milky Way, has a proper motion of just a few tenths of microarcseconds (van der Marel et al. 2019). Taking the remaining 53 063 (54 611 – 1 548) ALHAMBRA sources, we found 5 102 sources having *Gaia* counterparts in a 3 arcsec radius, out of which 3 774 are sources with non-zero proper motions, defining as such those sources fulfilling that, at least, one of the proper motion components is larger (in absolute value) than three times the associated error. Among them, 1 733 sources also fulfilled the conditions of having relative errors of less than 10 per cent in G and G_{RP} and less than 20 per cent in both proper motion components.

Of these 1 733 sources, 462 lie in the expected locus for dwarfs in a reduced proper motion diagram defined as

$$H_G = G + 5 \log \mu + 5, \quad (2)$$

where G is the *Gaia* apparent magnitude and μ is the total proper motion in mas yr^{-1} (Fig. 3). In this type of diagrams, proper motion is used as a proxy for distance assuming that nearby objects will have higher proper motions. Just as in an HRD, reduced proper motion diagrams have been shown to be excellent tools for segregating the various stellar populations (Dhital et al. 2010; Jiménez-Esteban, Caballero & Solano 2011; Lodieu et al. 2012; Zhang et al. 2013; Lodieu et al. 2017; Smart et al. 2017).

Among the 462 sources, 29 also fulfil the $G - G_{RP} > 1.3$ condition. We applied VOSA to this sample, keeping only those with $T_{\text{eff}} \leq 2900$ K. We ended up with just one object (ALHAMBRA 81481207114).

Regarding COSMOS, 678 sources satisfy the conditions on magnitudes and proper motion components, out of which 59 also fulfil the $G - G_{RP} > 1.3$ condition. After applying VOSA, we kept only one source with $T_{\text{eff}} \leq 2900$ K (COSMOS 690108).

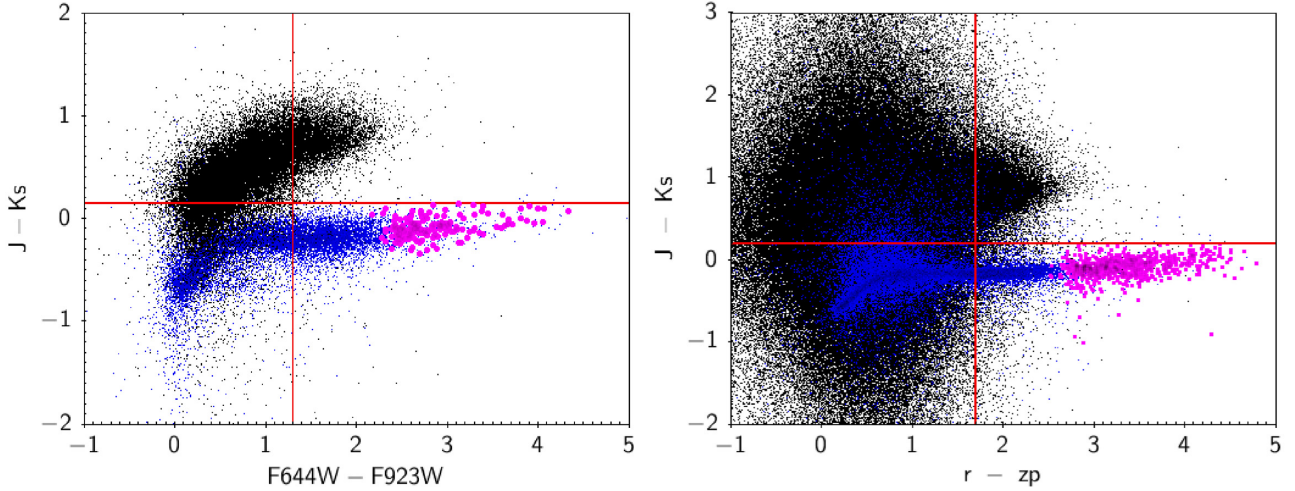


Figure 4. ALHAMBRA (left-hand panel) and COSMOS (right-hand panel) colour–colour diagrams. Black and blue dots represent galaxies and stars, respectively. The vertical and horizontal red lines mark the boundaries of the stellar and galactic locus. Pink bullets represent the 164 (30+1+133) ALHAMBRA and the 733 (1+1+731) COSMOS candidate UCDs.

2.4 Photometry

After applying the first two criteria (location in the HRD and reduced proper motion), only 3 281 sources (1 548 + 1 733, respectively) have been classified as stars in the ALHAMBRA survey. To discriminate between stars and galaxies in the remaining list of 51 330 (54 611 – 3 281) sources, we used the ALHAMBRA photometric information. We assigned a ‘true galaxy’ status to all objects with *Stellar_Flag* and *stell* in the range 0.0–0.1, and a ‘true star’ status to all objects with these flags in the range 0.9–1. After testing different combinations, we decided to use the $J - K_s$ versus $F644W - F923W$ colour–colour diagram to discriminate between the two types of sources. This is similar to the criterion used in fig. 9 of Strait (2015), but adapted to ALHAMBRA photometry.

Fig. 4 shows the ALHAMBRA and COSMOS ‘true star’ and ‘true galaxy’ objects in the colour–colour diagram. Following Strait (2015), the region in the colour–colour diagram fulfilling the following conditions,

$$F644W - F923W > 1.3,$$

$$J - K_s < 0.15, \quad (3)$$

is defined as the ‘ALHAMBRA true star locus free of contamination (< 1 per cent) by extragalactic object’.

Likewise, the region above $J - K_s > 0.15$ is defined as the extragalactic locus free of stellar contamination (< 1 per cent). The remaining region

$$F644W - F923W \leq 1.3$$

$$J - K_s \leq 0.15 \quad (4)$$

is occupied both by galaxies (42 per cent) and stars (58 per cent) and an efficient separation cannot be applied.

Using this criteria with the remaining 51 330 sources, we were able to classify 15 353 sources as galaxies, 1 402 as stars while 14 846 sources lie in the overlapping region between stars and galaxies and were not classified. The remaining 19 729 sources had bad photometry in any of the four filters and were not classified either.

According to the position in the colour–colour diagram of the UCDs found in the two previous sections, we define as candidate

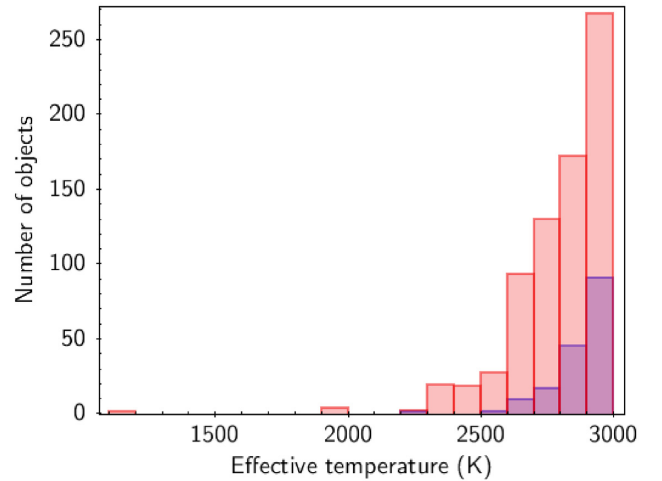


Figure 5. T_{eff} distribution of the candidate UCDs identified in COSMOS (red) and ALHAMBRA (blue).

UCD a stellar source with $F644W - F923W > 2.15$. A total of 272 sources passed this criterion. After applying VOSA, we kept 133 with $T_{\text{eff}} \leq 2900$ K.

Similarly, we selected all COSMOS sources with good photometry in the r, zp (Subaru) and J, K_s (ULTRAVISTA) bands and separate stars from galaxies in a $(J - K_s)$ versus $(r - zp)$ colour–colour diagram. We used the flags *TYPE* to separate stars from galaxies. The stellar locus was defined by the following region (Fig. 4):

$$r - zp \geq 1.7,$$

$$J - K_s \leq 0.2. \quad (5)$$

We found 1 220 sources fulfilling these criteria, out of which 731 have effective temperatures ≤ 2900 K. Adding the candidate UCDs found by the three searches (HRD, proper motion and colours) a total of 897 (164 ALHAMBRA + 733 COSMOS) sources is obtained.

Fig. 5 shows the distribution of effective temperatures of our 897 candidate UCDs. Most of them lie in the 2 600–2 900 K range while

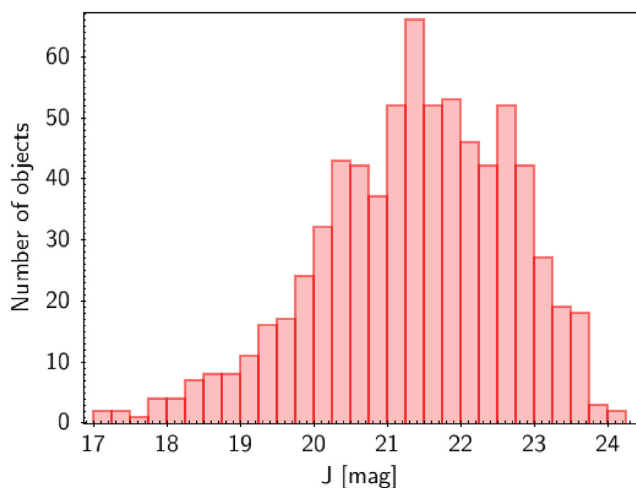


Figure 6. Distribution of the COSMOS candidate UCDs magnitudes. UltraVISTA DR2 *J*-band (AB) magnitude in a 3-arcsec aperture has been considered.

Table 2. COSMOS UCDs number counts. Ryan & Reid (2016) estimations have been computed considering both the thin and thick disc components and a sky area of 2 deg^2 .

Spectral type	Ryan & Reid (2016)	This work
M8–M9	100	120
L0–L9	72	43
T0–T5	1–2	1

the coolest object (COSMOS 752243 / CFBDS J100113+022622, a T5 BD) shows a $T_{\text{eff}} = 1100 \text{ K}$. The full list of 897 candidates is available online at the SVO archive of UCDs identified in ALHAMBRA and COSMOS (see Appendix A).

Different studies have been devoted to estimate the surface density of cool stars and BDs in deep extragalactic surveys, mainly to account for the degree of contamination by these objects due to their similar near-IR colours to high-redshift galaxies (e.g. Wilkins et al. 2014). In particular, Ryan & Reid (2016) calculate the surface density of UCDs in representative fields of the *James Webb Space Telescope*, including COSMOS. Using their tables 4–7 and fig. 6, and assuming $J = 23.5$ as COSMOS limiting magnitude (Fig. 6), we compared our list of candidate UCDs to their estimations finding a reasonable good agreement (Table 2).

3 KNOWN UCDS IN THE ALHAMBRA AND COSMOS FIELDS

In this section, we assess the fraction of known UCDs that have been recovered using our methodology. In particular, we looked for UCDs in SIMBAD (Wenger et al. 2000).

Using the SIMBAD TAP service,⁶ we chose objects having spectral types later than M7V or labelled as *BDs*. A total of 13 329 objects fulfilled these conditions.

To know how many of them lie in the region of the sky covered by ALHAMBRA and COSMOS, we took advantage of Aladin and the Multi-Object Coverage⁷ VO standard. Regarding ALHAMBRA,

a total of 193 SIMBAD UCDs lie in its field of view, but only 10 were really included in the ALHAMBRA catalogue. For COSMOS, there were 15 sources in the field of view, out of which 12 were in Laigle et al. (2016).

The efficiency of our search was estimated using the false-negative rate (number of known UCDs in SIMBAD that were not rediscovered in our search). For ALHAMBRA, nine of the objects were recovered by us. The remaining object (ALHAMBRA 81441106044) escaped from our search because of its low *stell* value (0.1). For COSMOS, seven objects were recovered while the remaining five escaped from our search due to different reasons: *TYPE* value different from 1 (2 sources), lack of *Ks* photometry (1 source) and $(J - Ks)$ colour slightly higher than 0.15 (2 sources).

4 SPECTROSCOPIC FOLLOW-UP

Another way to confirm the validity of our methodology to find new UCDs is to look for available spectroscopic information in public archives. We found spectra for 11 ALHAMBRA candidate UCDs in the SDSS DR16 archive⁸ using a 10 arcsec search radius. SDSS spectra cover the optical range ($\sim 3800\text{--}9200 \text{ \AA}$) with a resolving power $\lambda/(\Delta\lambda) = 1800$. Spectra were automatically reduced and assigned a spectral type by the SDSS pipeline software following Bolton et al. (2012). In all cases, the sources were classified as ‘stars’ with spectral types M5 (4), M6 (5), and M7 (2). We can see how the conservative value of T_{eff} adopted to select UCDs has a clear impact on the non-negligible number of contaminants (i.e. objects with spectral types earlier than M7 V). Two of the M6 objects (ALHAMBRA 81461309369 and ALHAMBRA 81473108856) were classified in SDSS as M6 III. However, the position of the first source in the HRD clearly indicates that this object is a dwarf. The second target was photometrically selected and we cannot conclude about its dwarf/giant nature. Regarding COSMOS we found spectroscopic information for two objects, COSMOS 247323 and COSMOS 601887, classified as M9 V and M6 V, respectively (Fig. 7). The list of objects with spectral type in SDSS is given in Table 3. One more object (ALHAMBRA 81422407651, classified as an M3 star) was found in LAMOST DR5.

Additionally, we got service mode time with LIRIS⁹ (Manchado et al. 1998) for two ALHAMBRA objects at the 4.2-m William Herschel Telescope in La Palma Observatory. The spectra of ALHAMBRA 81473108856 and ALHAMBRA 81473110590 were obtained on 2018 June 25–27 with a clear sky and a seeing of 0.9 arcsec for 81473108856 and 0.7 arcsec for 81473110590, respectively. The observations were reduced in the standard way (sky subtraction, flat-field division, extraction of the spectra, and wavelength calibration) with IRAF.¹⁰ The spectra have a wavelength coverage of $\sim 8890\text{--}23\,600 \text{ \AA}$ with a resolving power $\lambda/(\Delta\lambda) \approx 2600$.

We used a service of the Spanish VO¹¹ to gather observational and theoretical templates covering the M6–L8 spectral range. These templates were used to assess the UCD nature of the candidates. In particular, we used the NIRSPEC library (McLean et al. 2003, 2007). The templates were first convolved to match the LIRIS spectral resolution and the comparison was done by visual inspection.

⁸<https://dr16.sdss.org>

⁹<https://www.ing.iac.es/Astronomy/instruments/liris/>

¹⁰IRAF is distributed by the National Optical Observatory, which is operated by the Association of Universities for Research in Astronomy, Inc., under contract with the National Science Foundation.

¹¹<http://svo2.cab.inta-csic.es/theory/newov2/>

⁶<http://simbad.u-strasbg.fr:80/simbad/sim-tap>

⁷<http://ivoa.net/documents/MOC/index.html>

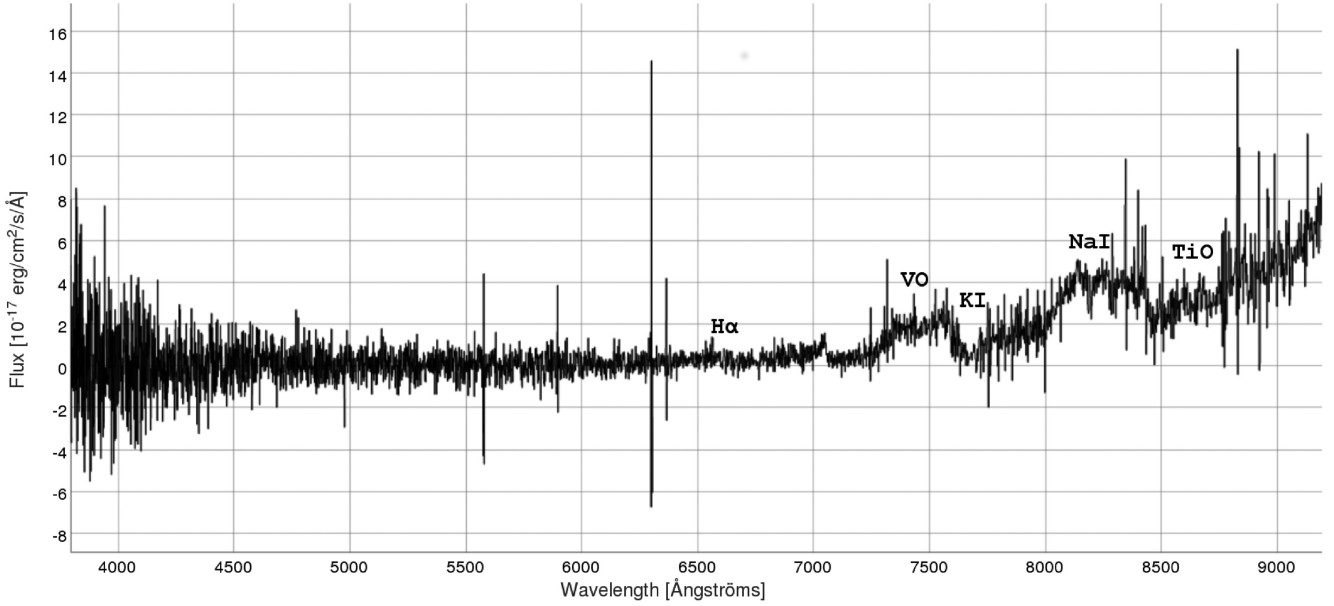


Figure 7. SDSS spectra of COSMOS 247323 (M9V). Together with the rest of SDSS spectra (12), it is available from the SVO archive (see the Appendix).

Table 3. Candidate UCDs with SDSS spectral types. The column *method* indicates whether the candidate has been selected using their position in the HRD or their colours (PHOT).

RA (ICRS, °)	Dec. (ICRS, °)	Survey	Source_id	ϖ (mas)	$\mu_{\alpha\cos\delta}$ (mas yr ⁻¹)	μ_{δ} (mas yr ⁻¹)	Gmag (mag)	Method	T_{eff}	Spectral type
37.0651	0.6742	ALHAMBRA	81421305057					PHOT	2600	M7
37.3364	0.5783	ALHAMBRA	81422407651	5.96	21.60	− 8.08	18.80	HRD	2900	M5
37.3496	0.6364	ALHAMBRA	81422405585	7.43	84.99	− 16.34	18.46	HRD	2900	M5
139.4752	45.9878	ALHAMBRA	81431401913	14.22	− 36.03	− 20.49	18.75	HRD	2700	M7
149.6099	2.2107	COSMOS	601887				19.87	PHOT	2900	M6
149.9955	1.65567	COSMOS	247323				20.61	PHOT	2500	M9
150.3242	2.3860	ALHAMBRA	81441108312				19.78	PHOT	2800	M6
188.4841	61.7146	ALHAMBRA	81451310113	5.52	− 8.67	− 34.86	18.98	HRD	2900	M5
213.3649	52.8089	ALHAMBRA	81462203395	12.30	5.87	− 45.38	17.79	HRD	2800	M6
214.0596	52.1862	ALHAMBRA	81461309369	7.57	25.29	− 50.40	18.90	HRD	2900	M6III
214.6764	52.7097	ALHAMBRA	81461107375	2.86	− 6.64	8.33	20.15	HRD	2900	M5
214.9342	52.3238	ALHAMBRA	81461402862	7.08	− 33.87	19.14	18.33	HRD	2800	M6
243.7100	54.5900	ALHAMBRA	81473108856				21.14	PHOT	2600	M6III

For visual comparison, we plot the LIRIS spectra together with those of the NIRSPEC library in the *Y* and *J* bands, which is where our targets have the best signal-to-noise ratio ranging from ~ 30 to ~ 40 (Fig. 8). The presence of the *K* I doublet at 1.168 and 1.177 μm clearly indicates that our targets are UCDs. We defer to a later paper the detailed analysis of these spectra and additional follow-up spectra of UCDs that we plan to obtain for preparation of the Euclid mission.

5 SIMULATIONS OF ULTRACOOL DWARF DETECTIONS IN THE EUCLID WIDE SURVEY

This decade the Euclid Space Mission will cover 15 000 deg² of the extragalactic sky with just one single epoch (the Euclid wide survey) and 40 deg² in three selected regions that will be observed repeatedly during the lifetime of the mission (6 yr).

The COSMOS field is likely to be selected as a calibration field for *Euclid*, and hence the analysis of UCDs considered in this work could be used as a reference.

The requirements for *Euclid* were stated in the Red Book (Laureijs et al. 2011). In this work, an updated version of the Euclid filter transmission passbands¹² has been adopted as follows: photometric sensitivity 24.5 mag. (AB) in VIS passband (0.55–0.9 μm), and 24 mag. (AB) in three NIR passbands, *Y* (0.945–1.231 μm), *J* (1.159–1.587 μm), and *H* (1.510–2.000 μm), and slit-less spectroscopic sensitivity of 21 mag. (AB) at spectral resolution of 250 over the wavelength range 1.25–1.85 μm . The corresponding sensitivities for the deep survey are 2 mag deeper.

The simulation parameters are the following: Log-normal mass function with α parameter = 0.5 (Chabrier 2005), star-formation rate

¹²<http://svo2.cab.inta-csic.es/theory/fps/index.php?&gname=Euclid>

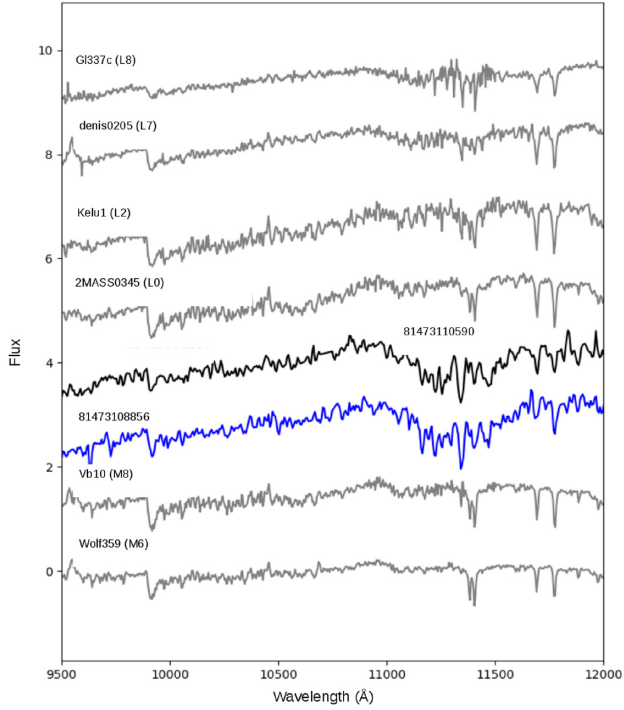


Figure 8. Comparison of the LIRIS spectra of two of our ALHAMBRA UCD candidates with template spectra from the NIRSPEC library.

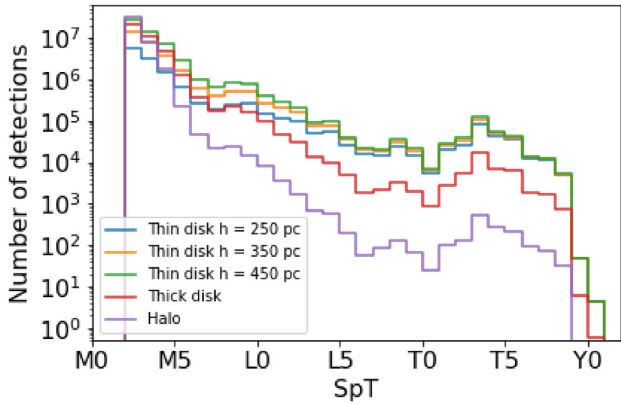


Figure 9. Simulated number counts of UCDs detected by the Euclid wide survey (15000 deg²) in the NISP *J* band for a constant galactic latitude of 45° for all objects.

from Aumer & Binney (2009), evolutionary models from Burrows et al. (1993), spectral type versus absolute magnitudes and T_{eff} from Pecaut & Mamajek (2013), disc scale heights from 250 to 450 pc (Ryan & Reid 2016), although a value around 450 pc appears more likely from recent results by Sorahana, Nakajima & Matsuoka (2019) and Carnero Rosell et al. (2019), and constant galactic latitude at 45° for all objects and total survey area of 15000 deg².

The most sensitive filter to UCDs in the Euclid wide survey will be the *J* band as shown in Fig. 9. About two million L dwarfs, one million T dwarfs and a handful of Y dwarfs are expected to be detected in the thin disc for a scale height of 450 pc (green line). The corresponding numbers are about a factor of 2 lower for a scale height of 250 pc (blue line), about a factor of 10 lower for the thick disc population

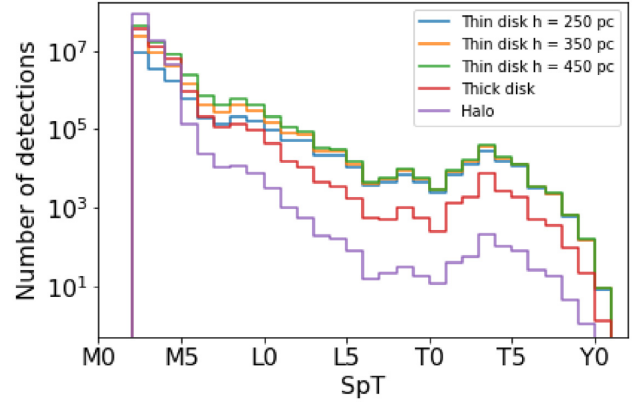


Figure 10. Same as Fig. 9, but for the NISP *Y* band.

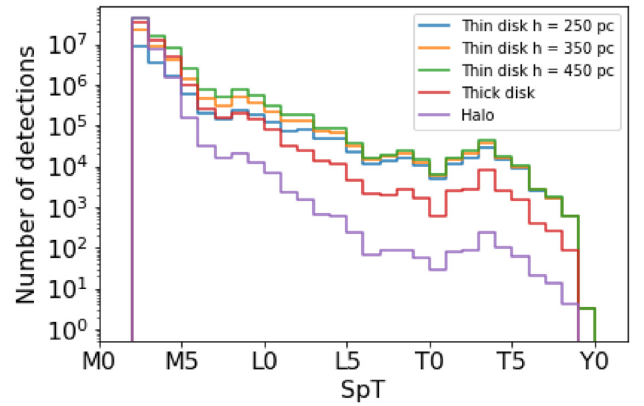


Figure 11. Same as Fig. 9, but for the NISP *H* band.

(red line), and about a factor of 500 lower for the halo (purple line). For comparison, simulations of UCD number counts in the *Y* and *H* bands are shown in Figs 10 and 11, respectively. A very large number of UCDs (of the order of 1 million objects) are expected to be detected in the three NISP passbands. This is important because, as shown in this work and in other works such as Deacon (2018), Holwerda et al. (2018), it is not enough to detect a UCD in one or two filters to identify it as such. Parallaxes, proper motions and/or multicolours are needed. Ideally, all of them are required for secure identification.

The VIS instrument will provide higher spatial resolution than NISP, which will allow to resolve hundreds of UCD binaries. Simulations of UCD number counts in the VIS filter are shown in Fig. 12. The numbers of UCDs expected to be detected in the VIS-band are more than a factor of 100 less than in the *J* band, particularly for late-T dwarfs.

In the Euclid photometric catalogues, the availability of colours for UCDs is going to be provided mainly by the NISP instrument. The colour method will be based on *Y-J* versus *J-H* colour–colour diagrams. The UCDs identified in this work will be useful to calibrate those diagrams with known UCDs. It will also be useful to cross identify Euclid point sources detected in the *J* band with the NEOWISE catalogue in the *W1* and *W2* bands to find T and Y dwarfs.

The proper motion and parallax methods of UCD identification can be applied in the Euclid deep fields and in the calibration fields.

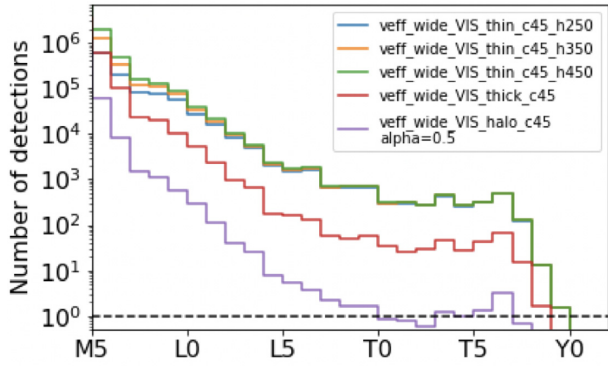


Figure 12. Same as Fig. 9, but for the Euclid VIS-band.

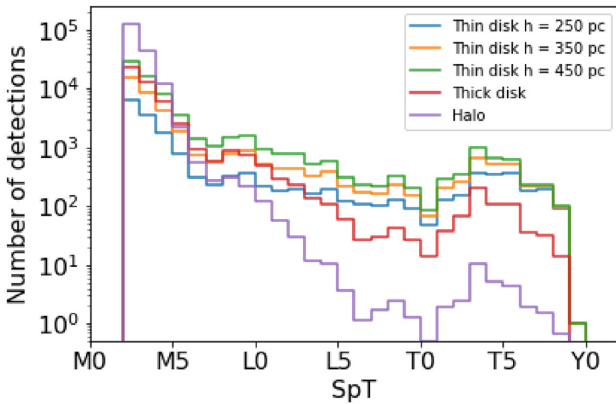


Figure 13. Same as Fig. 9 but for the Euclid deep surveys (40 deg^2) in the NISP *J* band.

In Fig. 13, the predicted number counts of UCDs in the total area expected to be covered by the deep fields are presented. The number of T dwarfs that could be identified in the Euclid deep fields by proper motions in the *J* band may be of order of a few thousands. These objects will be selected independently from their colours, and hence they will provide useful feedback to the colour methods used to select UCDs in the wide-field survey.

6 CONCLUSIONS

Using a VO methodology, we have built a catalogue of 897 candidate UCDs found in the ALHAMBRA and COSMOS extragalactic surveys. In total, 16 of them were already known in SIMBAD. Our primary goal in this paper was not to carry out a detailed analysis on the properties of the found candidates but to define and assess a search methodology to be used for deeper and larger surveys like Euclid, whose excellent sensitivity makes it an ideal resource for the discovery of new UCDs, including BDs with very low effective temperatures.

The use of different approaches based on parallaxes, proper motions, and colours tends to minimize the drawbacks and biases associated to the search of ultracool objects: photometric-only selected samples may leave out peculiar UCDs not following the canonical trend in colour–colour diagrams and they can also be affected by extragalactic contamination. Proper motion searches may ignore objects with small values of projected velocity in the plane of

the sky. Regarding parallax-based searches, they will be limited to the brightest objects with parallax values from *Gaia*.

With the help of the VOSA we estimated effective temperatures for our candidate UCDs. They range from 1100 to 2900 K with the great majority of the objects in the 2600–2900 K range. We also compared the number of candidate UCDs found in the COSMOS field with theoretical estimations (Ryan & Reid 2016), finding a good agreement. The high success ratio recovering known UCDs demonstrates the robustness of our procedure, and the consistency with predicted counts of UCDs in the COSMOS fields indicates that the VO-based procedures described in this paper are reliable to efficiently mine forthcoming wide and deep surveys for new UCDs. We found that our choice of 2900 K as an upper effective temperature limit in our selection is not restrictive enough to prevent somewhat earlier M dwarfs (M4–M6 V) from contaminating the sample of UCD candidates and will be taken into account in subsequent studies.

Last but not least, we present simulated number counts of UCDs detected in the Euclid wide and deep fields, and we discuss the applicability of the methods of UCD detection used in this work.

ACKNOWLEDGEMENTS

This research has made use of the Aladin sky atlas developed at CDS, Strasbourg Observatory, France. This publication makes use of VOSA, developed under the Spanish Virtual Observatory project supported from the Spanish MICIU through grant AyA2017-84089. This research has been partly funded by the Spanish State Research Agency (AEI) Project MDM-2017-0737 at Centro de Astrobiología (CSIC-INTA), Unidad de Excelencia María de Maeztu. EM was supported by grant AYA2015-69350-C3-1-P. NL was supported by grant AYA2015-69350-C3-2-P. This work has made use of data from the European Space Agency (ESA) mission *Gaia*,¹³ processed by the *Gaia* Data Processing and Analysis Consortium (DPAC).¹⁴ We also extensively made use of TOPCAT (Taylor 2005) and STILTS (Taylor 2006) as well as the VizieR and SIMBAD services, both operated at CDS, Strasbourg, France.

DATA AVAILABILITY STATEMENT

The data underlying this paper are available at http://svo2.cab.inta-csic.es/vocats/alhambra_cosmos/.

REFERENCES

- Allard F., Homeier D., Freytag B., 2012, *Phil. Trans. R. Soc. Ser. A*, 370, 2765
- Aumer M., Binney J. J., 2009, *MNRAS*, 397, 1286
- Bayo A., Rodrigo C., Barrado Y Navascués D., Solano E., Gutiérrez R., Morales-Calderón M., Allard F., 2008, *A&A*, 492, 277
- Bolton A. S. et al., 2012, *AJ*, 144, 144
- Burrows A., Hubbard W. B., Saumon D., Lunine J. I., 1993, *ApJ*, 406, 158
- Carnero Rosell A. et al., 2019, *MNRAS*, 489, 5301
- Chabrier G., 2005, in Corbelli E., Palle F., eds, *Astrophysics and Space Science Library* Vol. 327, *The Initial Mass Function: From Salpeter 1955 to 2005*. Springer, Dordrecht, p. 41
- Cuby J. G., Saracco P., Moorwood A. F. M., D’Odorico S., Lidman C., Comerón F., Spyromilio J., 1999, *A&A*, 349, L41

¹³<https://www.cosmos.esa.int/gaia>

¹⁴<https://www.cosmos.esa.int/web/gaia/dpac/consortium>

- Deacon N. R., 2018, *MNRAS*, 481, 447
- Dhital S., West A. A., Stassun K. G., Bochanski J. J., 2010, *AJ*, 139, 2566
- Gaia Collaboration et al., 2018, *A&A*, 616, A10
- Gillon M. et al., 2017, *Nature*, 542, 456
- Helling C. et al., 2008, *MNRAS*, 391, 1854
- Henry T. J., Jao W.-C., Subasavage J. P., Beaulieu T. D., Ianna P. A., Costa E., Méndez R. A., 2006, *AJ*, 132, 2360
- Holwerda B. W. et al., 2018, *A&A*, 620, A132
- Jiménez-Esteban F. M., Caballero J. A., Solano E., 2011, *A&A*, 525, A29
- Jones H. R. A., Tsuji T., 1997, *ApJ*, 480, L39
- Kirkpatrick J. D. et al., 1999, *ApJ*, 519, 802
- Laigle C. et al., 2016, *ApJS*, 224, 24
- Laureijs R. et al., 2011, preprint ([arXiv:1110.3193](https://arxiv.org/abs/1110.3193))
- Liu M. C., Wainscoat R., Martín E. L., Barris B., Tonry J., 2002, *ApJ*, 568, L107
- Lodieu N., Dobbie P. D., Deacon N. R., Venemans B. P., Durant M., 2009, *MNRAS*, 395, 1631
- Lodieu N., Espinoza Contreras M., Zapatero Osorio M. R., Solano E., Aberasturi M., Martín E. L., 2012, *A&A*, 542, A105
- Lodieu N., Espinoza Contreras M., Zapatero Osorio M. R., Solano E., Aberasturi M., Martín E. L., Rodrigo C., 2017, *A&A*, 598, A92
- Luri X. et al., 2018, *A&A*, 616, A9
- McLean I. S., McGovern M. R., Burgasser A. J., Kirkpatrick J. D., Prato L., Kim S. S., 2003, *ApJ*, 596, 561
- McLean I. S., Prato L., McGovern M. R., Burgasser A. J., Kirkpatrick J. D., Rice E. L., Kim S. S., 2007, *ApJ*, 658, 1217
- Manchado A. et al., 1998, in Fowler A. M., ed., SPIE Conf. Ser., Vol. 3354, Infrared Astronomical Instrumentation. SPIE, Bellingham, p. 448
- Martin E. L., Rebolo R., Zapatero-Osorio M. R., 1996, *ApJ*, 469, 706
- Martin E. L., Basri G., Delfosse X., Forveille T., 1997, *A&A*, 327, L29
- Martín E. L., Cabrera J., Martioli E., Solano E., Tata R., 2013, *A&A*, 555, A108
- Moles M. et al., 2008, *AJ*, 136, 1325
- Molino A. et al., 2014, *MNRAS*, 441, 2891
- Pecaut M. J., Mamajek E. E., 2013, *ApJS*, 208, 9
- Rebolo R., Martin E. L., Basri G., Marcy G. W., Zapatero-Osorio M. R., 1996, *ApJ*, 469, L53
- Ryan R. E. J., Reid I. N., 2016, *AJ*, 151, 92
- Smart R. L., Marocco F., Caballero J. A., Jones H. R. A., Barrado D., Beamín J. C., Pinfield D. J., Sarro L. M., 2017, *MNRAS*, 469, 401
- Sorahana S., Nakajima T., Matsuoka Y., 2019, *ApJ*, 870, 118
- Strait V., 2015, American Astronomical Society Meeting Abstracts #225. p. 336.51
- Taylor M. B., 2005, in Shopbell P., Britton M., Ebert R., eds, ASP Conf. Ser. Vol. 347, Astronomical Data Analysis Software and Systems XIV. Astron. Soc. Pac., San Francisco, p. 29
- Taylor M. B., 2006, in Gabriel C., Arviset C., Ponz D., Solano E., eds, ASP Conf. Ser. Vol. 351, Astronomical Data Analysis Software and Systems XV. Astron. Soc. Pac., San Francisco, p. 666
- van der Marel R. P., Fardal M. A., Sohn S. T., Patel E., Besla G., del Pino A., Sahlmann J., Watkins L. L., 2019, *ApJ*, 872, 24
- Wenger M. et al., 2000, *A&AS*, 143, 9
- West A. A. et al., 2011, *AJ*, 141, 97
- Wilkins S. M., Stanway E. R., Bremer M. N., 2014, *MNRAS*, 439, 1038
- Zhang Z. H. et al., 2013, *MNRAS*, 434, 1005

APPENDIX: VIRTUAL OBSERVATORY COMPLIANT, ONLINE CATALOGUE

In order to help the astronomical community on using our catalogue of candidate UCDs, we developed an archive system that can be accessed from a webpage¹⁵ or through a Virtual Observatory ConeSearch

The archive system implements a very simple search interface that allows queries by coordinates and radius as well as by other parameters of interest. The user can also select the maximum number of sources (with values from 10 to unlimited) and the number of columns to return (minimum, default, or maximum verbosity). The result of the query is a HTML table with all the sources found in the archive fulfilling the search criteria (Fig. A1). The result can also be downloaded as a VOTable or a CSV file. Detailed information on the output fields can be obtained placing the mouse over the question mark located close to the name of the column. The archive also implements the SAMP¹⁶ (Simple Application Messaging) Virtual Observatory protocol. SAMP allows VO applications to communicate with each other in a seamless and transparent manner for the user. This way, the results of a query can be easily transferred to other VO applications, such as, for instance, Topcat.

¹⁵http://svo2.cab.inta-csic.es/vocats/alhambra_cosmos/

¹⁶<http://www.ivoa.net/documents/SAMP>



The SVO archive of ultracool dwarfs identified in ALHAMBRA and COSMOS.

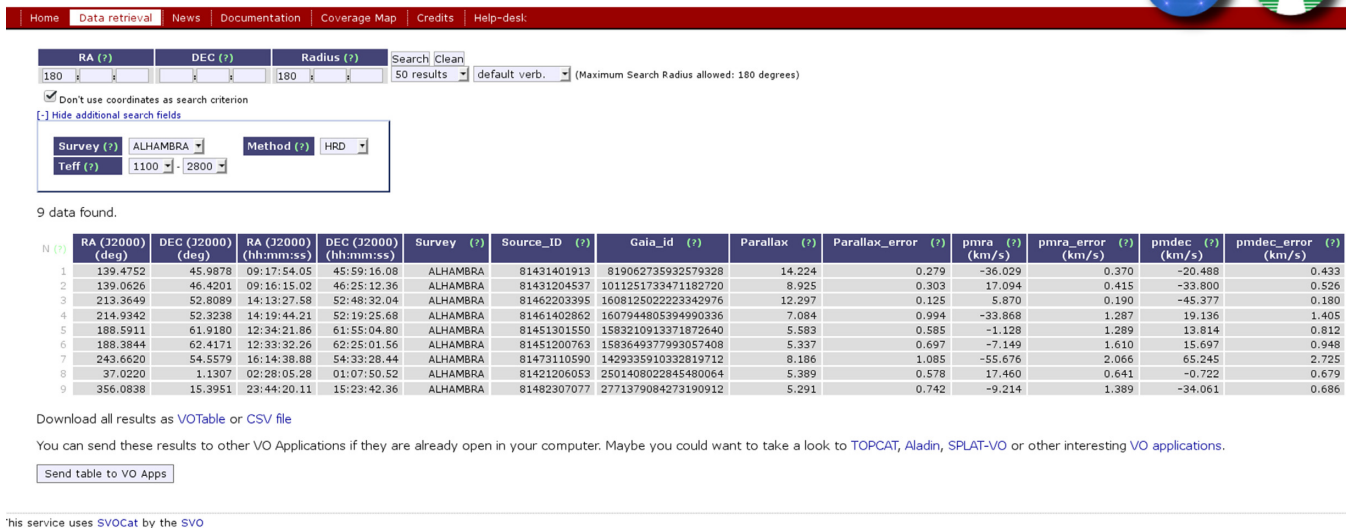


Figure A1. Result from a query in the SVO archive of UCDs identified in ALHAMBRA and COSMOS.

This paper has been typeset from a \LaTeX file prepared by the author.